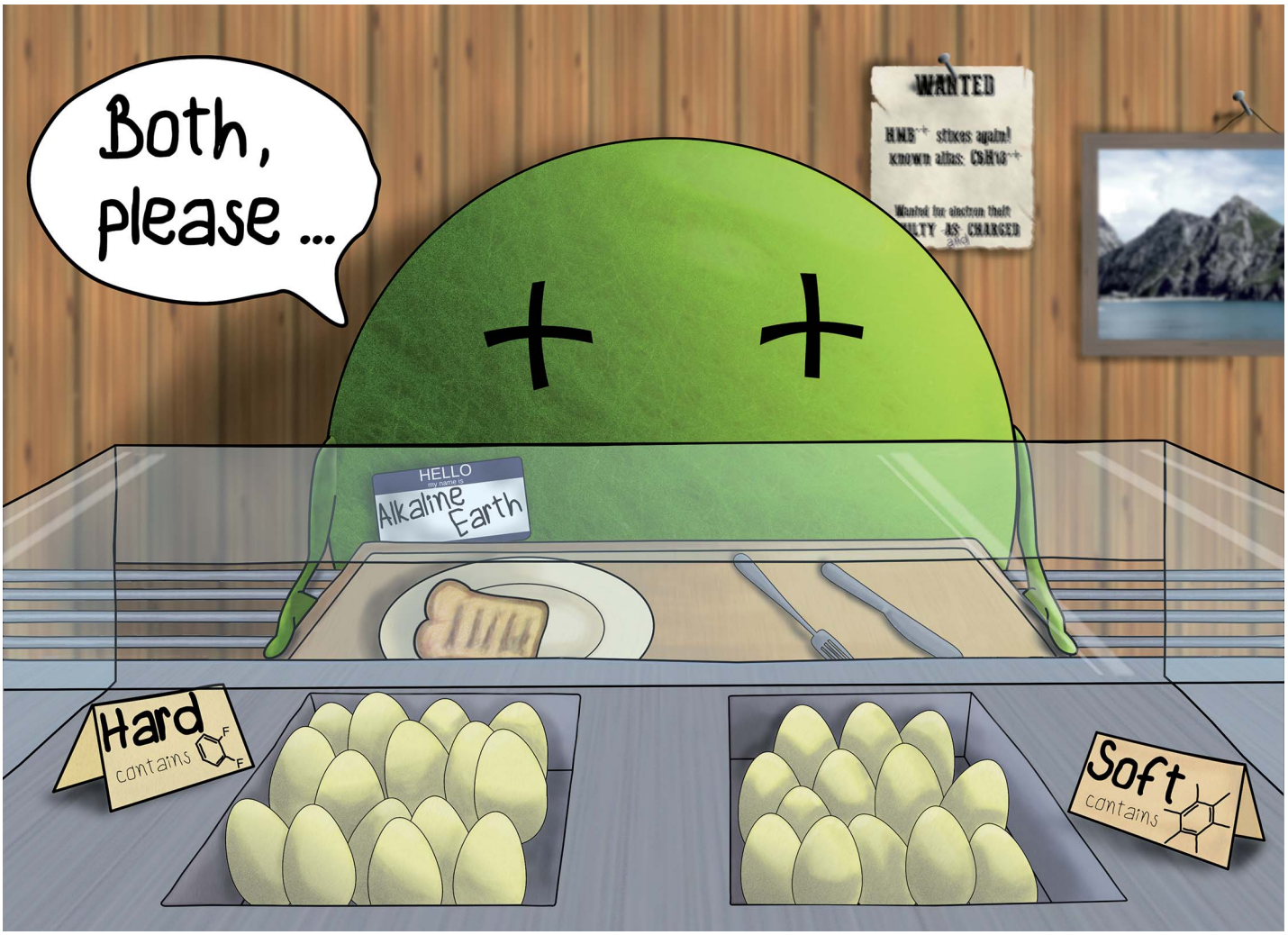

Showcasing research from Professor Krossing's laboratory, Institute for Inorganic and Analytical Chemistry, University of Freiburg, Germany.

Soft interactions with hard Lewis acids: generation of mono- and dicationic alkaline-earth metal arene-complexes by direct oxidation

The key to success for the synthesis of the title compounds – unsupported mono- and dicationic heavier alkaline earth metal-arene complex salts – is the ligand-forming oxidising agent: the hexamethylbenzene radical cation ([HMB]$^{+}$) paired with the weakly coordinating anions [Al(OR^{F})$_4$]$^{-}$ and [(^{F}RO)$_3$Al-F-Al(OR^{F})$_3$]$^{-}$ (R^{F} = C(CF$_3$)$_3$). The half-sandwich complexes form when treating elemental alkaline earth metals (Ca, Sr, Ba) with [HMB][WCA] difluorobenzene solutions. These unprecedented structures show extremely high and hard Lewis acidities in terms of their Fluoride Ion Affinities and possess a peculiar soft/hard coordination environment supplied by η^6-coordinated hexamethylbenzene and κ^2-F coordinated difluorobenzene molecules.

As featured in:

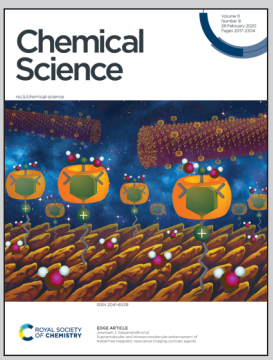

See Marcel Schorpp and Ingo Krossing, *Chem. Sci.*, 2020, **11**, 2068.

ROYAL SOCIETY OF CHEMISTRY

rsc.li/chemical-science

Registered charity number: 207890

Chemical Science

ROYAL SOCIETY OF CHEMISTRY

EDGE ARTICLE

View Article Online
View Journal | View Issue

Cite this: *Chem. Sci.*, 2020, **11**, 2068

All publication charges for this article have been paid for by the Royal Society of Chemistry

Received 10th December 2019
Accepted 12th January 2020

DOI: 10.1039/c9sc06254h

rsc.li/chemical-science

Soft interactions with hard Lewis acids: generation of mono- and dicationic alkaline-earth metal arene-complexes by direct oxidation†

Marcel Schorpp and Ingo Krossing *

The synthesis of the first unsupported dicationic arene complexes of calcium and strontium $[(\eta^6\text{-HMB})AE(o\text{DFB})_4]^{2+}$ is reported (HMB = hexamethylbenzene; AE = alkaline earth metal; *o*DFB = *ortho*-difluorobenzene). They were prepared by direct oxidation of the elemental metals employing the ligand-forming radical cation salt [HMB][WCA] as an oxidant (WCA = $[Al(OR^F)_4]$ or $[\mu F\text{-}\{Al(OR^F)_3\}_2]$; $R^F = C(CF_3)_3$). In addition, monocationic η^6-HMB complexes of calcium, strontium and barium supported by coordination of the monodentate anion $[F\text{–}Al(OR^F)_3]^-$ are reported. In all examples, almost undistorted η^6-HMB coordination is observed with rather short M-$arene_{centroid}$ distances approaching those observed with the isoelectronic but negatively charged pentamethylcyclopentadienyl ligand. The structure and bonding, thermodynamic stability and Lewis acidity (fluoride/hydride ion affinities, FIA/HIA) of the generated complexes were assessed by DFT methods. It followed that the gaseous dications $[(\eta^6\text{-HMB})AE(o\text{DFB})_4]^{2+}$ are extremely hard Lewis acids that retain FIAs close to superacidity in solution.

While coordination of anionic 6π-aromatics such as group 2 metallocenes has been known for more than 60 years, the coordination of neutral arenes to heavier Alkaline Earth (AE) metals is scarce and neutral arene complexes of AE metal dications without a supporting ligand framework are still unprecedented.[1] Hitherto, mainly the enforced coordination of flanking aryl rings of anionic polydentate ligand scaffolds in neutral or monocationic complexes was observed. The first structurally characterized example of an isolated arene coordinating to a heavier AE metal dates back to 2001. Here Ba^{2+} formed neutral dinuclear complexes with a very strong σ-chelating porphyrinogen. Its central metal is perfectly η^6 coordinated by arenes (benzene, toluene, naphthalene, and durene).[2] Formally cationic complexes were later discovered within the tightly bound $(BaCl_2Ga)_\infty$ coordination-network of $[Ba(\eta^6\text{-}C_6H_6)_2(GaCl_4)_2]_\infty$. Related dimeric motifs $[Ba(C_7H_8)_2(MEt_4)_2]_2$ with tightly bound formal $[MEt_4]^-$ (M = Al, Ga) counterions were reported.[3] The directed binding of isolated arenes to the hard and highly Lewis acidic metal centers was only observed within rigid $[(ligand)AE(\eta^x\text{-arene})]^{0,+}$ pockets. Thus, Hill and Harder paired monoanionic chelating beta-diketiminate ligands (NacNac) with Mg and Ca to form the complex salts [M(NacNac)][WCA] (where WCA = $[B(C_6F_5)_4]$ or $[Al(OR^F)_4]$ with $OR^F = -OC(CF_3)_3$). They include highly Lewis acidic cations that are capable of coordinating benzene, toluene, *m*-xylene, and mesitylene, as well as the generally poorly coordinating silyl ethers.[4,5] In addition, cationic Lewis base-free $[M(NacNac)][B(C_6F_5)_4]$ complexes compete with $B(C_6F_5)_3$ in their Lewis acidity. By addition of difluorobenzene, a $[Mg(NacNac)(1,4\text{-}F_2C_6H_4)_3]^+$ complex cation with κ^1-F–M interactions is generated. It was also possible to isolate further complex cations with rather unconventional ligands for AE metal chemistry, for example triphenylphosphine and 3-hexyne adducts. Due to their high Lewis acidity, the π-electron density of the hexyne-adduct is highly polarized allowing for activation and subsequent attack of the C–C multiple bond.[6,7] Related is the reaction between [Ca(NacNac)][WCA] and Al^I(NacNac) in the presence of benzene. Originally the Lewis donor–acceptor complex was aimed for, but instead reduction of benzene to an alumina-norbornadiene derivative was observed.[8] These results generated renewed interest in group 2 chemistry and their possible application in catalysis to exploit their pronounced Lewis acidity. Useful examples include monocationic and neutral AE complexes that were used in the transfer hydrogenation or hydrosilylation of alkenes and imines. Concomitantly, the underlying reactivity of intermediary and selectively generated M-hydride species has been elucidated.[7,9]

Inspired by the recent synthesis of isolated cationic mono-arene group 13 complexes $[M^I(HMB)]^+$ (M = Ga, In) with

Institut für Anorganische und Analytische Chemie, Freiburger Materialforschungszentrum (FME), Universität Freiburg, Albertstr. 21, 79104 Freiburg, Germany. E-mail: krossing@uni-freiburg.de

† Electronic supplementary information (ESI) available: Experimental details, procedures, weights, 1D- and 2D-NMR spectra, IR spectra and powder diffraction patterns of the reactions, and details of the quantum chemical calculations together with crystallographic details. CCDC 1969777–1969784. For ESI and crystallographic data in CIF or other electronic format see DOI: 10.1039/c9sc06254h

the ligand-forming oxidant $[HMB]^{+\bullet}[Al(OR^F)_4]^-$ (eqn (1), HMB = hexamethylbenzene),[10] we were interested in transferring this methodology to group 2, *i.e.* the formation of unsupported mono-/bis(arene)-complexes by direct oxidation of the elemental metals as shown in eqn (2).

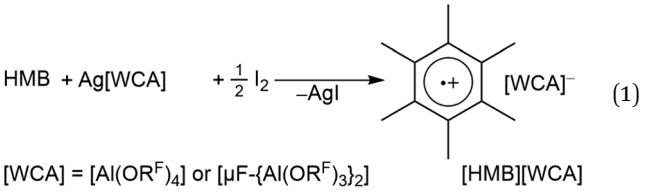

(1)

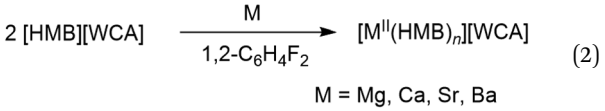

(2)

Results and discussion

Orienting investigations towards Mg and Ca salts using $[HMB][Al(OR^F)_4]$

The first reactions between magnesium and the ligand-forming oxidant $[HMB][Al(OR^F)_4]$ in *ortho*-difluorobenzene (*o*DFB) were futile; instead the deep red color attributed to the HMB radical slowly faded over weeks, while the only isolable products were the already reported[10] long-term degradation products of $[HMB]^{+\bullet}$: $[C_6Me_7]^+$ and the cycloaddition product of $[HMB]^{+\bullet}$ and *o*DFB (see Scheme 1a). However, upon spiking the reaction mixture with a few drops of MeCN, immediate loss of the deep red color was observed. Single crystals suitable for X-ray diffraction analysis revealed a hexacoordinate acetonitrile magnesium salt, $[Mg(MeCN)_6][Al(OR^F)_4]_2$ **1** (see Scheme 1b & Fig. S1†). The formal potential of the oxidant $[HMB]^{+\bullet}$ is therefore most likely not high enough to oxidize magnesium in non-polar media and only upon addition of the donor solvent MeCN does the formation of the stable hexacoordinate Mg^{II} salt give the thermodynamic driving force for the reaction to proceed.

The reaction between less noble calcium and $[HMB][Al(OR^F)_4]$ in *o*DFB proceeds *via* color loss over five days. By layering the filtrate of the reaction mixture with *n*-pentane, we obtained a crystalline material of the form $[Ca(HMB)(oDFB)_2\{f\text{-}al\}][Al(OR^F)_4]$ **2** ($[f\text{-}al]^- = [F\text{–}Al(OR^F)_3]^-$, see Scheme 1c, Fig. 1a & Table 1).

The cationic part constitutes Ca in the +II oxidation state ion-paired with an anionic $[f\text{-}al]^-$ moiety, giving an overall monocationic complex. The $[f\text{-}al]^-$ fragment herein stems from a decomposition reaction of the $[Al(OR^F)_4]^-$ counterion, presumably proceeding *via* fluoride abstraction by the generated Ca^{2+} species, loss of OC_4F_8 epoxide and re-coordination to the liberated $Al(OR^F)_3$ Lewis acid – a well-documented degradation path of this anion with extreme electrophiles like small silylium ions.[11,12] Half of the by electron transfer (ET) generated neutral HMB is η^6-bound to the central Ca with a Ca arene distance of $d_{Ca\text{-centroid}} = 2.459(6)$ Å (structures and metric data in Fig. 1 and Table 1). This is the shortest coordination of an isolated neutral arene reported in the literature (*cf.* $[Ca(NacNac)(C_6H_6)][Al(OR^F)_4]$ $d_{Ca\text{-centroid}} = 2.596$ Å (ref. 13)). Moreover, it is in the range of Ca-pentamethylcyclopentadienide (Cp*) distances with the anionic $[Cp^*]^-$ ligand in $CaCp^*(ODipp)(THF)_3$ (Dipp = 2,6-iPr-C_6H_3), (avg. $d_{Ca\text{-centroid}} = 2.453$ Å (ref. 14)) and only by 0.1 Å longer as in $CaCp^*_2$ (avg. $d_{Ca\text{-centroid}} = 2.351$ Å (ref. 15)). The remaining space in the coordination sphere around Ca in **2** is filled by coordination of two difluorobenzene molecules with κ^2-F–M coordination mode with rather short M–F contact distances ranging from $d_{Ca\text{–}F} = 2.415(7)$ to $2.483(7)$ Å. Generally, the coordination of halobenzenes *via* their halogen atoms is scarce and κ^2-F coordination of difluorobenzene was only structurally characterized in $[M^{III}Cp^*_2(oDFB)][BPh_4]$ (M = Sc, Ti). This underlines the high

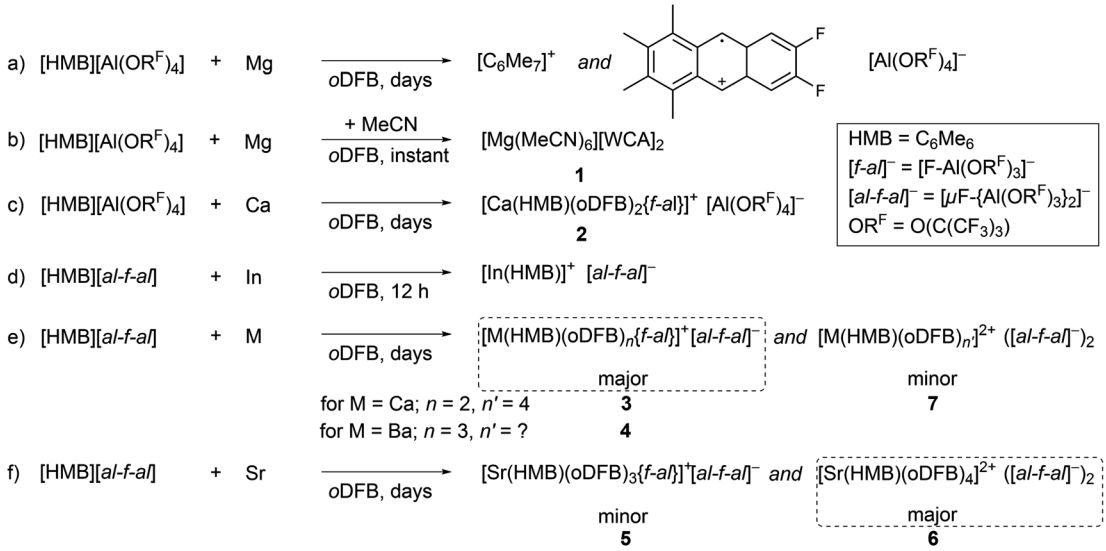

Scheme 1

Lewis acidity of the central calcium atom.[16] The shortest M–F distance with $d_{Ca-F} = 2.185(7)$ Å is formed with the coordinated $[f\text{-}al]^-$ moiety, with further M–F interactions with peripheral CF_3 fluorine atoms of this anionic ligand ($d_{Ca-F} = 2.620(8)$ Å). The Al–F and Al–O bonds ($d_{Al-F} = 1.714(8)$ & avg. $d_{Al-O} = 1.704(9)$ Å) are well in the range of the reported bond lengths for $[f\text{-}al]^-$.[12]

Switching to the fluoride-bridged anion $[\mu F\text{-}\{Al(OR^F)_3\}_2]^-$; reactions with Ca–Ba

Synthesis and first application of [HMB][*al-f-al*]. In order to overcome anion decomposition and to possibly stabilize truly dicationic AE complexes, the anion was exchanged for the larger and more stable (towards highly electrophilic species) fluoride bridged anion $[\mu F\text{-}\{Al(OR^F)_3\}_2]^-$ ($[al\text{-}f\text{-}al]^-$) for all further reactions.[12,17,18] To investigate the compatibility of the chosen oxidant with this anion, a solution of [HMB][*al-f-al*] was prepared by an analogous synthetic protocol to eqn (1), but changing the anion. The deep red *o*DFB solution was filtered from precipitated AgI and analyzed by NMR spectroscopy showing no anion decomposition even after days at ambient temperature. When reacting the prepared [HMB][*al-f-al*] with thinly sheeted indium metal, fast color loss was observed (see Scheme 1d). Crystals suitable for single crystal X-ray structure determination (scXRD) were grown by layering the reaction mixture with *n*-pentane. The obtained crystalline solid consists of the expected salt [In(HMB)][*al-f-al*] (see Fig. S8†), proving the compatibility of the chosen anion with this oxidant.

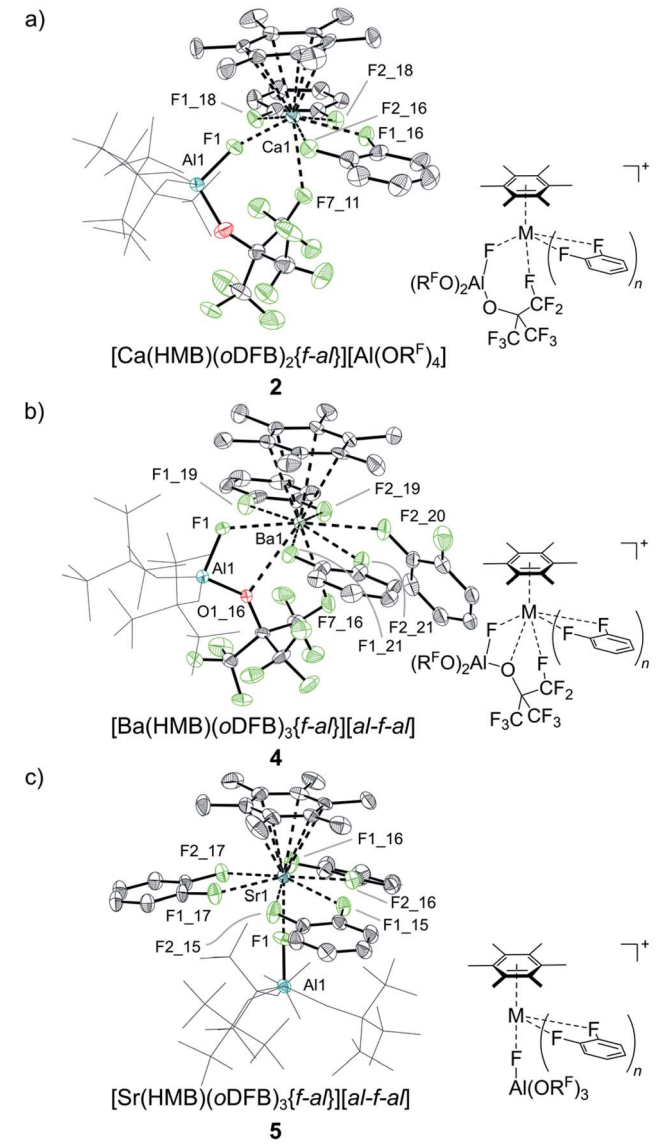

Fig. 1 Molecular structures of the cationic parts of (a) **2**, (b) **3**, and (c) **5** (due to disorder only the majority component of bound $[f\text{-}al]^-$ is shown for clarity). Counterions and protons are omitted and parts of $[f\text{-}al]^-$ are drawn as wireframes for clarity. Thermal displacement ellipsoids are shown at 50% probability.

Reaction with Ca and Ba after incorporation of the $[f\text{-}al]^-$ anion. Reaction procedures for the oxidation of the AE metals were adapted and [HMB][*al-f-al*] reacted with calcium (see Scheme 1e). After complete color loss (5 days), the reaction mixture was filtered and single crystals were obtained by layering the reaction mixture with *n*-pentane. Their molecular structure shows an almost identical coordination environment in the cationic part as described above for **2** and the salt was identified as [Ca(HMB)(oDFB)$_2${*f-al*}][*al-f-al*] **3**. There is also a notable additional interaction between Ca and one of the OR^F side arms with interaction with a peripheral F–CF_2-group as well as a short Ca–O contact distance of avg. $d_{Ca-O} = 3.05(2)$ Å. The latter causes a slight elongation of the respective Al–O bond to $d_{Al-O} = 1.77(2)$ Å (for the molecular structure see Fig. S9,† and for bond metric data see Table 1).

Similar results have been obtained when reacting the heavier congener Ba with [HMB][*al-f-al*], yielding [Ba(HMB)(*o*DFB)$_3${*f-al*}][*a-f-al*] **4** (see Scheme 1e and Fig. 1b). Again HMB is η^6-coordinated with a Ba-centroid distance of $d_{Ba\text{-centroid}} = 2.850(3)$ Å (*cf.* $BaCp^*_2$ $d_{Ba\text{-centroid}} = 2.733$ Å,[15] BaCp*X $d_{Ba\text{-centroid}} = 2.752$ Å;[20] X = C(N(iPr)$_2$)N(H)iPr). The cationic structure of **4** is closely related to that of **3**, except for an additional, κ^1-F bound *o*DFB (with Ba–F distances ranging from $d_{Ba-F} = 2.791(4)$ Å to 2.939(5) Å) accounting for the larger metal atom. The [*f-al*] moiety is bound similarly to **3** with a short Ba–F contact distance of $d_{Ba-F} = 2.589(4)$ Å, as well as coordination to oxygen on one of the OR^F sidearms ($d_{Ba-O} = 2.941(5)$ Å). It is noteworthy that the bound $[f\text{-}al]^-$ moiety in **3** and **4** does not stem from fluoride abstraction but rather dissociation of the anion. This may be understood as the result of a competition between the two Lewis acids AE^{2+} and $Al(OR^F)_3$ for the Lewis basic anionic $[f\text{-}al]^-$ fragment. We note that the dissociation of $[al\text{-}f\text{-}al]^-$ to give the coordinated $[f\text{-}al]^-$ anion and the free Lewis acid $Al(OR^F)_3$ may be supported by complexation of the latter with *o*DFB giving the known adduct (*o*DFB)$Al(OR^F)_3$.[21] Therefore, this route provides a controlled synthesis of complexes **3** and **4**.

Reactions with Sr. We therefore presumed that the aimed for free dicationic AE complexes are too electrophilic for isolation with the anions used herein, and similar results were expected for strontium with an intermediate reactivity between Ca and Ba. However, from the reaction between Sr and [HMB][*al-f-al*] (see Scheme 1f) again single crystals were obtained by layering of the decolorized reaction mixture with *n*-pentane. Two sorts of crystalline materials with different habitus were formed on

Table 1 Selected interatomic distances for complexes **2** to **7** in Å given as ranges and averages due to multiple cationic moieties in the asymmetric unit together with bond valences {v.u.}, according to I.D. Brown for complexes **3** to **7**.[19] Al–$O_{avg.}$ for O atoms showing no interaction to the central AE element

		2	**3**	**4**	**5**	**6**	**7**
	M=	Ca	Ca	Ba	Sr	Sr	Ca
HMB	M–C_{range}	2.82(1)–2.88(1)	2.787(9)–2.906(9)	3.134(7)–3.193(7)	2.997(6)–3.016(6)	2.997(3)–3.025(3)	2.813(3)–2.916(3)
	M–$C_{avg.}$	2.84(1)	2.843(9)	3.170(7)	3.006(5)	3.015(3)	2.872(3)
*o*DFB	M–F_{range}	2.415(7)–2.483(7)	2.445(6)–2.503(6)	2.791(4)–2.939(5)	2.625(3)–2.703(3)	2.595(2)–2.799(2)	2.360(2)–2.565(2)
			{0.17–0.20; Σ = 0.72}	{0.11–0.20; Σ = 0.83}	{0.15–0.20; Σ = 1.03}	{0.15–0.21; Σ = 1.35}	{0.14–0.25; Σ = 1.13}
	M–$F_{avg.}$	2.441(7)	2.471(6)	2.865(4)	2.661(3)	2.683(2)	2.466(2)
	C–F_{range}	1.36(1)–1.39(1)	1.376(3)–1.379(3)	1.364(9)–1.389(9)	1.362(5)–1.393(5)	1.376(2)–1.386(2)	1.371(3)–1.392(3)
	C–$F_{avg.}$	1.38(1)	1.378(3)	1.378(9)	1.375(5)	1.381(2)	1.381(3)
[*f-al*]$^-$	M–F	2.185(7)	2.189(6)	2.589(4)	2.338(3)	—	—
			{0.39}	{0.34}	{0.42}		
	Al–F	1.714(8)	1.712(6)	1.705(4)	1.699(3)	—	—
			{0.64}	{0.65}	{0.66}		
	M–O	—	3.05(2)	2.941(5)	—	—	—
			{0.05}	{0.17}			
	Al–$O_{avg.}$	1.704(9)	1.69(2)	1.709(5)	1.70(1)	—	—
	Al–$O_{M\ bound}$	—	1.77(2)	1.769(5)	—	—	—

different sides in the layering tube. The major product crystallized as block shaped crystals, while the minor product crystallized as a few small needle type crystals, both suitable for single crystal X-ray diffraction analysis. The needle shaped crystals again showed a related coordination of [*f-al*]$^-$ to the central strontium atom (see Fig. 1c), yielding the monocationic complex ([Sr(HMB)(*o*DFB)$_3${*f-al*}][*al-f-al*] **5**. Note that here, in contrast to Ca and Ba, the [*f-al*]$^-$ fragment is bound opposite to the HMB ligand with no additional close Sr–anion contact other than in the Sr–F–Al interaction. This mode leaves three *o*DFB molecules coordinated in an equatorial plane around the central Sr atom. Yet the major product, the block shaped crystals, revealed the targeted truly free dicationic Sr HMB complex salt ([Sr(HMB)(*o*DFB)$_4$][*al-f-al*]$_2$ **6**; Fig. 2a). It shows again an η^6-bound HMB with a Sr–arene distance of $d_{Sr\text{-centroid}} = 2.665(1)$ Å as well as coordination of four *o*DFB molecules bound κ^2 with Sr–F distances ranging from 2.595(2) to 2.799(2) Å. As such, **6** represents the first free AE^{2+} arene complex without a supporting ligand framework.

NMR investigations. NMR spectra of the isolated crystalline material containing **5** and **6** underlined the subjective impression of **6** being the major product as only 7% [*f-al*]$^-$ was detected by ^{19}F-NMR spectroscopy. Intrigued by these findings, we were interested to see if we could detect similar species for both Ca and Ba. Therefore, NMR spectroscopic investigations of reaction mixtures were conducted. As both [*f-al*]$^-$ and [*al-f-al*]$^-$ show easily distinguishable resonances in ^{19}F NMR spectra, the ratio between the two anionic moieties should be in accordance with the obtained molecular structure, *i.e.* 1 : 1 for **3** and **4**. However, in all collected samples a distinct excess of the fluoride-bridged anion was detected ([*f-al*]$^-$: [*al-f-al*]$^-$; 1 : 2.1 for **3** and 1 : 1.7 for **4**), which is not accounted for by cationic trace impurities from HMB radical degradation reactions. NMR spectra of isolated crystalline materials from reactions with both Ca and Ba showed similar outcomes. Furthermore, the sum of both anionic moieties and HMB, as determined by referencing to *o*DFB as an internal standard, shows a 2 : 1 ratio. Since free HMB is soluble in both *o*DFB and pentane, and the respective ^{13}C resonances of the quaternary ring carbon in HMB show a significant downfield shift for all samples by $\Delta\delta = 15$ ppm compared to those of free HMB, it is likely that the excess fluoride bridged anion is part of a second dicationic HMB complex containing two intact fluoride bridged anions. Yet, all attempts to selectively synthesize or crystallize the minor products have failed and only by a serendipitous finding could a dicationic Ca complex, [Ca(HMB)(*o*DFB)$_4$][*al-f-al*]$_2$ **7** (see Scheme 1e and Fig. 2b), be isolated from the layering ampoule showing a similar coordination to the already-described **6** (for bond metric data see Table 1).

Relation between mono- and dicationic structures. Comparison of interatomic distances between the two Ca and Sr containing complexes, **3** and **7**, and **5** and **6**, respectively, shows an increase in the avg. M–C bond lengths and a decrease of the M–F_{oDFB} contact distances noticeably for Ca and marginally for Sr when going from mono- to dicationic complexes. Although sterically encumbered, the binding of [*f-al*]$^-$ satisfies the electrostatic frustration around the metal center allowing for closer

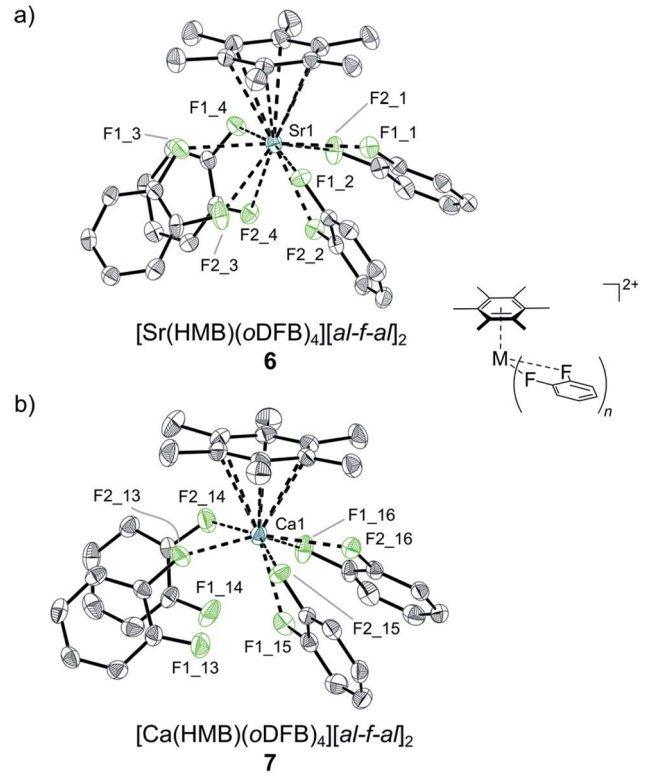

Fig. 2 Molecular structures of the cationic parts of (a) **6** and (b) **7**. Counterions and protons are omitted for clarity. Thermal displacement ellipsoids are shown at 50% probability.

contact with the bound arene moiety. Comparison of the sums of the M–(F, O) bond valences (see Table 1) in **3**, **4** and **5** around the central M gives values Σ(v.u.) for Ca = 1.20, Sr = 1.45 and Ba = 1.45. For the dicationic species **6** and **7** the bond valence sums are rather similar with Ca = 1.13 and Sr = 1.35, showing – due to the absence of the strongly bound $[f\text{-}al]^-$ anion at $0.34_{Ca}/0.39_{Sr}$ v.u. – an increased interaction with the *o*DFB ligands. For the M–C contact distances, no parameters are available and thus they cannot be addressed. However, they presumably make up the difference to the expected valence of the AE metals of v.u. = 2. For all of the obtained complexes **3** to **7** an elongation of the C–F bond lengths in bound *o*DFB is observable ranging from 0.02 to 0.05 Å (see Table 1; *cf.* $d_{C-F} = 1.345(8)$ taken from κ^1 bound *o*DFB in **3** and **7**) with the greatest effect for the two dicationic complexes **6** and **7**, showing activation of the aromatic C–F bonds in all complexes. Similar effects on the C–F bond length have been observed when fluorobenzene is coordinated to other Lewis acid fragments *e.g.* $Al(OR^F)_3$ with an elongation by 0.09 Å.[22]

Since with identical reaction procedures only Sr^{2+} complex **6** was easily isolable as the major product, we were intrigued to understand the underlying thermodynamics, as this suggests an equilibrium state between dicationic and monocationic $[f\text{-}al]^-$ bound complexes. However, the generation of $[f\text{-}al]^-$ from $[al\text{-}f\text{-}al]^-$ inevitably generates one equivalent of $Al(OR^F)_3$, the fate of which is unclear. Its fluoro- and difluorobenzene adducts are known and rather soluble in *o*DFB, but are only marginally stable at room temperature and were not clearly assignable by NMR spectroscopy.[21] Attempts to generate the dications by abstraction of $[f\text{-}al]^-$ from **4** with the stable $Al(OR^F)_3$ equivalent and strong Lewis acid $Me_3Si\text{–}F\text{–}Al(OR^F)_3$ (fluoride ion affinity FIA = 458 kJ mol^{-1}) did not increase the $[al\text{-}f\text{-}al]^-$ content, underlining the tight ion-pairing of the anionic $[f\text{-}al]^-$ moiety. We conclude that the concentration of unbound $[f\text{-}al]^-$ must be very minimal, making a true equilibrium and thus the reaction of free $[f\text{-}al]^-$ with $Me_3Si\text{–}F\text{–}Al(OR^F)_3$ to give $[al\text{-}f\text{-}al]^-$ and Me_3SiF unlikely. Therefore, the formation of the monocationic complexes is irreversible and apparently only slightly favored over the formation of the dication in **7** and maybe **6**. Furthermore, the resonances in ^{19}F-NMR spectra attributable to M-bound $[f\text{-}al]^-$ moieties at about −130 to −152 ppm are distinctly low field-shifted compared to those of "free" $[f\text{-}al]^-$ (*e.g.* in $[CPh_3][f\text{-}al]$, $\delta = -186.1$ ppm; in $Ag[f\text{-}al]$, $\delta = -189.9$ ppm) and are more comparable to that in $Me_3Si\text{–}F\text{–}Al(OR^F)_3$ ($\delta = -156.2$ ppm), suggesting tight bonding of this moiety. Additionally, the binding of the anionic $[f\text{-}al]^-$ differs between the isolated complexes **3**, **4** and **5** as the ^{19}F-NMR chemical shift of aluminum bound fluorine in $[f\text{-}al]^-$ is distinctly low-field shifted by $\Delta\delta = 20$ ppm in the barium complex ($\delta = -130.3$ ppm) **4**, compared to **3** ($\delta = -151.5$ ppm) and **5** ($\delta = -149.3$ ppm). This suggests a very tight bonding interaction of this moiety in **4**.

DFT calculations

Thermodynamic considerations. In order to rationalize the gathered experimental findings, isodesmic model reactions for DFT analysis (BP86-D3(BJ)/def-SV(P) with solvation computed by the COSMO module, see eqn (3) were devised. They started from the obtained structural data. The (missing) molecular structure of the dicationic barium complex was derived from the structural data of **6** as $[Ba(HMB)(oDFB)_4]^{2+}$. For these dications, the abstraction of $[f\text{-}al]^-$ from the fluoride bridged anion supported by *o*DFB coordination at the Lewis acid $Al(OR^F)_3$ is favorable in solution for all three AE metals (eqn (3). The difference in $\Delta_R G^\circ_{(solv)}$ is small and lies within the error of the method but is apparently not linear when descending down the group. For strontium, the formation of the monocationic complex is least favorable, while barium again shows an increased tendency for this reaction. As the fate of the $Al(OR^F)_3$ generated during the formation of the $[f\text{-}al]^-$ bound complexes is unknown, the respective known[21] *o*DFB adduct was included to provide a balanced equation.‡ Thus, it appears that all compounds are thermodynamic products and only Sr dication **6** is the kinetic product that is metastable at RT in *o*DFB solution against further reaction to the $[f\text{-}al]^-$ coordinated product.

$$[M(HMB)(oDFB)_n]^{2+} + [al\text{-}f\text{-}al]^- \longrightarrow [M(HMB)(oDFB)_m\{f\text{-}al\}]^+ + oDFB{\cdot}Al(OR^F)_3 + (n\text{-}m\text{-}1)\ oDFB \quad (3)$$

M = Ca, n = 4, m = 2, $\Delta_R G^\circ_{(solv)}$ = −39.5 kJ/mol
M = Sr, n = 4, m = 3, $\Delta_R G^\circ_{(solv)}$ = −26.7 kJ/mol
M = Ba, n = 4, m = 3, $\Delta_R G^\circ_{(solv)}$ = −35.2 kJ/mol

To evaluate the reaction energies for the exchange of the X-type ligand $[f\text{-}al]^-$ between the different mono- and dicationic AE complexes, they were investigated according to eqn (4a–c).

$$[Ca(L)]^{2+}_{\mathbf{7^{2+}}} + [Sr(L)(X)]^{+}_{\mathbf{5^{+}}} \underset{\{-15.6\}}{\overset{(-37.4)}{\rightleftharpoons}} [Ca(L)(X)]^{+}_{\mathbf{3^{+}}} + [Sr(L)]^{2+}_{\mathbf{6^{2+}}} \quad (4a)$$

$$[Ca(L)]^{2+}_{\mathbf{7^{2+}}} + [Ba(L)(X)]^{+}_{\mathbf{4^{+}}} \underset{\{-7.7\}}{\overset{(-3.5)}{\rightleftharpoons}} [Ca(L)(X)]^{+}_{\mathbf{3^{+}}} + [Ba(L)]^{2+} \quad (4b)$$

$$[Sr(L)]^{2+}_{\mathbf{6^{2+}}} + [Ba(L)(X)]^{+}_{\mathbf{4^{+}}} \underset{\{8.6\}}{\overset{(33.9)}{\rightleftharpoons}} [Sr(L)(X)]^{+}_{\mathbf{5^{+}}} + [Ba(L)]^{2+} \quad (4c)$$

$X = [F\text{-}Al(OR^F)_3]^-$, $L = HMB(oDFB)_n$

$(\Delta_R G^\circ_{(gas)})$ and $\{\Delta_R G^\circ_{(solv)}\}$ in kJ/mol

Abstraction of $[f\text{-}al]^-$ by $[M(HMB)(oDFB)_4]^{2+}$ from $[M'(HMB)(oDFB)_n\{f\text{-}al\}]^+$ is exergonic for M = Ca and M′ = Sr (-15.6 kJ mol^{-1}; eqn (4a)) and Ba (-7.7 kJ mol^{-1}; eqn (4b)), while the abstraction for M = Sr and M′ = Ba is counterintuitively endergonic (+8.6 kJ mol; eqn (4c)). Although all of the obtained reaction energies are rather close, a trend supporting the experimental findings is visible. The increased stability of the monocationic Ba complex $\mathbf{3}^+$ in comparison to the monocationic Sr complex $\mathbf{5}^+$ causes the abstraction of $[f\text{-}al]^-$ by $\mathbf{7}^{2+}$ to be more exergonic for the latter, and the abstraction by $\mathbf{6}^{2+}$ to be endergonic for the former. These findings are also backed by NMR spectroscopic investigations as described above, showing stronger coordination by $[f\text{-}al]^-$ in **4**. To understand the stability of isolated dicationic complexes **7** and especially **6**, a dismutation of the strontium complex **6** to hypothetical $[Sr(HMB)_2]^{2+}$ and $[Sr(oDFB)_8]^{2+}$ was modeled (see eqn (5)). This transformation was found to be unfavorable by 176 kJ mol^{-1} in $\Delta_R G^\circ$ ($\Delta_R G^\circ_{(solv)} = 98$ kJ mol^{-1}), underlining the stability of this unique coordination environment.

$$2\,[Sr(HMB)(oDFB)_4]^{2+} \underset{\{98\}}{\overset{(176)}{\longrightarrow}} [Sr(HMB)_2]^{2+} + [Sr(oDFB)_8]^{2+} \quad (5)$$

$(\Delta_R G^\circ_{(gas)})$ & $\{\Delta_R G^\circ_{(solv)}\}$ in kJ/mol

Structure and bonding. To understand the bonding situation in the obtained complexes, NBO, PABOON, and AIM population analyses were performed. Scheme 2 contains calculated electron densities at bond and cluster critical points (BCP & CCP) ρ_{CP} (in e Å^{-3}) (left) together with the partial charges (right). All of the dicationic complexes $\mathbf{7}^{2+}$, $\mathbf{6}^{2+}$ and $[Ba(HMB)(oDFB)_4]^{2+}$ show equal behavior with a linear shift from Ca–Ba, increasing the positive charge on the central metal while the charge on the bound HMB decreases. The partial positive charge on the bound aromatic implies depletion of π-electron density by bonding into the metal's empty $(n-1)$d-orbitals. The accessibility of the AE metal's d-orbitals for bonding in general was only recently verified by generation of respective neutral AE octacarbonyl species.[23] Yet, they show metal-to-ligand back bonding to the empty π* MO in CO, instead of the ligand-to-metal donation suggested here. The critical points M–C BCP and CCP in the M(HMB) subunit show a similar linear decrease when descending down group 2.

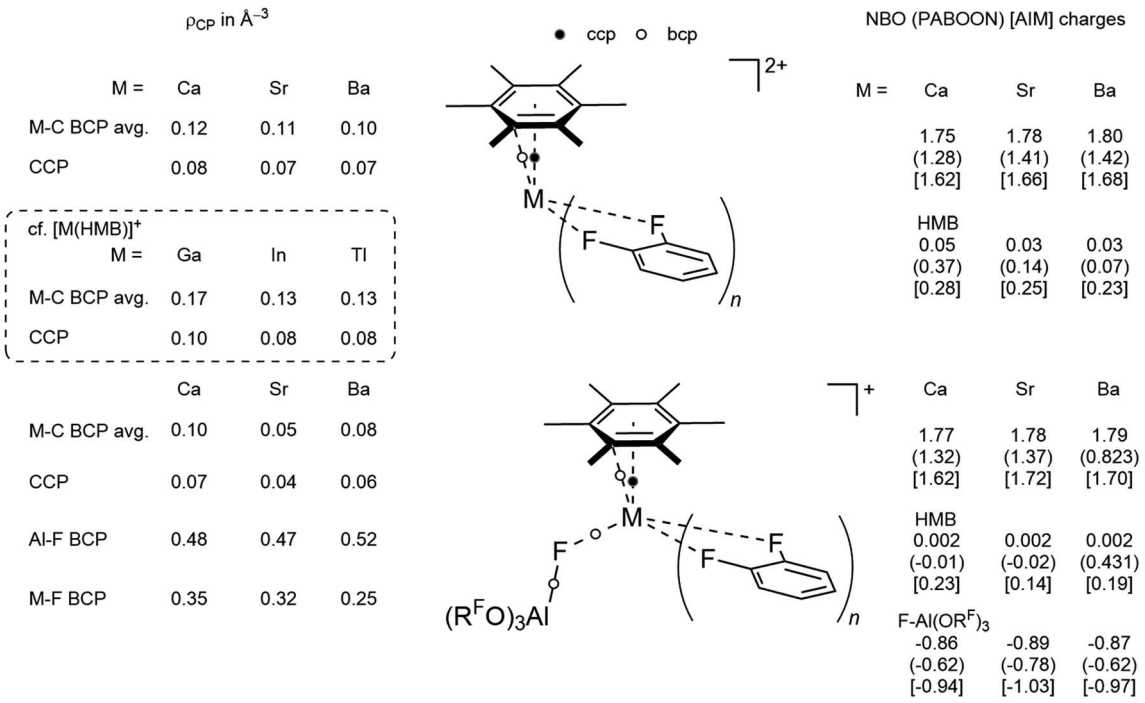

Scheme 2 Population analysis by NBO,[24] PABOON[25] and AIM[26] and electron density at bond and cluster critical points.

For the monocationic complexes, the same behavior is observed for Ca and Sr in $\mathbf{3}^+$ and $\mathbf{5}^+$. However, the positive charge on the central Ba in $\mathbf{4}^+$ decreases noticeably for both PABOON and AIM compared to the Sr complex $\mathbf{5}^+$, while the charge on bound HMB increases, suggesting more π-donation by HMB in this complex, in agreement with the best 5d acceptor capacity of Ba^{2+}. AIM analysis of the electron density residing at critical points reveals an increase for the M–C BCP and CCP located in the center of the Ba(HMB) subunit with decreasing electron density on the BCP of the M–F bond. The presence of the CCP in the M(HMB) subunit allows for its description as a nido-cluster analogous to the reported cationic group 13 HMB complexes $[M(HMB)]^+$ (ρ_{CP}(CCP) = 0.10 (Ga), 0.08 (In) and 0.08 e Å^{-3} (Tl)).

Investigation of the Lewis acidity

According to Gutmann and Beckett. The empirical Gutmann–Beckett method was chosen for the determination of the Lewis acidity.[27] For this, **4** was exemplarily reacted with one equivalent of $OPEt_3$. NMR spectroscopic investigations revealed five resonances in the ^{31}P NMR between δ = 84.8 and 64.1 ppm with a major resonance at δ = 81.7 ppm. Re-collection of the same sample after 14 days revealed a further change of the composition in ^{31}P-NMR as well as complete degradation of the $[al\text{-}f\text{-}al]^-$ counterion (along with competing formation of Et_3PO–$Al(OR^F)_3$ complexes). The determination of Lewis acidity by this method was therefore deemed non-applicable to the complexes described herein. We note that similar experiences were earlier reported when trying to evaluate AE based NacNac systems.[5]

Ion affinities. Therefore, the calculated fluoride and hydride ion affinities (FIA & HIA) were chosen as a measure for Lewis acidity. FIAs were calculated in the gas phase as well as in CH_2Cl_2 as a solvent medium (ε_r = 8.93) using COSMO[28] and referenced to the respective ion affinity of TMS^+ determined at the G3 level of theory (FIA = 958 kJ mol^{-1}; HIA = 959 kJ mol^{-1}).[18,29] It should be noted that the Lewis acidity of ionic systems is heavily attenuated by solvation and the last few years have provided a large number of examples for this.[29–31] Out of those investigations, the evaluation of the Lewis acidity by FIA/HIA calculations including solvation corrections to CH_2Cl_2 as solvent evolved as the most frequent. In agreement with this convention, we calculated the FIA/HIA values in CH_2Cl_2 rather than our standard solvent *o*DFB. The XIAs (X = F, H) were determined according to eqn (4) and are shown in Table 2.

$$[LA]^{n+} + TMS\text{-}X \xrightarrow{\Delta H_r} [LA\text{-}X]^{(n-1)+} + [TMS]^+$$

$$XIA = -\Delta_r H + XIA_{ref};\ XIA_{solv} = XIA - \{E_{solv}(LA\text{-}X) - E_{solv}(X^-) - E_{solv}(LA)\}$$

XIA; XIA_{solv} in kJ mol^{-1} with X = F, H (6)

All of the dicationic complexes $\mathbf{7}^{2+}$, $\mathbf{6}^{2+}$ and $[Ba(HMB)(oDFB)_4]^{2+}$ show expectedly very high FIAs in both the gas phase (923–879 kJ mol^{-1}) and in solution (316–283 kJ mol^{-1}), comparable only to those of a recently reported also dicationic phosphorandiylium $[R_3P]^{2+}$ species (FIA = 904 kJ mol^{-1}; FIA_{solv} = 318 kJ mol^{-1}).[31] Although the gas phase values exceed those of $B(C_6F_5)_3$ (FIA = 456 kJ mol^{-1}; FIA_{solv} = 240 kJ mol^{-1}) and SbF_5 (FIA = 494 kJ mol^{-1}; FIA_{solv} = 330 kJ mol^{-1}) – allowing for their declaration as Lewis superacids – their solvated FIAs in DCM are considerably lower. However, they are still much higher than that of $B(C_6F_5)_3$ and comparable in size to that of SbF_5 or $Al(OR^F)_3$ (FIA = 539 kJ mol^{-1}; FIA_{solv} = 323 kJ mol^{-1}). These solvated values underline the above-mentioned competition between AE^{2+} and $Al(OR^F)_3$ around the $[f\text{-}al]^-$ moiety.

Table 2 Determined fluoride (FIA) and hydride ion affinities (HIA) for presented complexes. Determined at the BP86-D3(BJ)/def-SV(P) level of theory. Solvation effects determined by use of the COSMO module[a]

Compound	FIA	FIA_{solv}	HIA	HIA_{solv}
$B(C_6F_5)_3$	456	240	485	158
SbF_5	494	330	n.a.	n.a.
$Al(OR^F)_3$	539	323	487	165
$\mathbf{7}^{2+}$	923	316	804	99
$\mathbf{6}^{2+}$	893	296	780	86
$[Ba(HMB)(oDFB)_4]^{2+}$	879	283	772	86
$\mathbf{3}^+$	654	234	538	22
$\mathbf{5}^+$	625	191	510	−17
$\mathbf{4}^+$	565	159	453	−35

[a] HIA not applicable to SbF_5 due to instability of SbF_5H.[18]

The calculated XIAs decrease when descending down group 2, although non-linearly. The difference between Sr and Ba containing complexes **5** & **4** is in both cases smaller than the gap between Ca and Sr containing complexes **3** & **5**. By contrast, the calculated HIAs are not as pronounced as the FIA values and especially the solvated HIAs are rather small and in some cases even exothermic. This is in line with the Pearson hard character of the cations.

The experimental findings together with data gathered from DFT analysis allow for interpretation of the stability of the complexes found. The monocationic Ca complex is predominantly formed over **7** because of the very high Lewis acidity of the smallest central atom in this series. When going down the group this effect should lessen, in line with the isolation of the almost exclusively formed dicationic strontium complex **6**. A similar reactivity would be expected for the even less polarizing larger barium. However, here again the monocationic complex **4** is predominantly formed. NMR and DFT analysis revealed tighter bonding of the $[f\text{-}al]^-$ moiety and higher stability of **4**, respectively. The decreased charge on the central barium suggests higher covalent character in Ba–F–Al and especially Ba–HMB bonds. However, only the latter is backed by electron density analysis by AIM theory.

Conclusion

By use of the ligand-forming oxidant [HMB][WCA] we were able to generate a series of mono- and dicationic AE metal arene complexes $[(\eta^6\text{-HMB})M(oDFB)_n\{f\text{-}al\}]^+$ (M = Ca, Sr, Ba) and $[(\eta^6\text{-HMB})M(oDFB)_4]^{2+}$ (M = Ca, Sr) by direct oxidation of the

elemental metals. Thus far, no evidence for generation of the single oxidation products, the respective $AE^{(+I)}$ complexes, was observed – even at lower temperature. It is unclear, if the generation of the respective $AE^{(+II)}$ is due to overoxidation of $AE^{(+I)}$ species in solution or its disproportionation. For oxidative synthesis of such low valent AE complexes further studies concerning the type and sterics of the employed ligand and chosen oxidant have to be performed. The highly Lewis acidic AE metal centers show a polarized soft interaction with the η^6-coordinated HMB, while the rest of the coordination sphere is filled with hard interactions with coordinated *o*DFB and in the case of the monocationic complexes [*f-al*]$^-$. The modeled dismutation of dicationic **6** to hypothetical $[Sr(HMB)_2]^{2+}$ and $[Sr(oDFB)_8]^{2+}$ was shown to be unfavorable in $\Delta_R G^\circ$, underlining the stability of this unique mixed hard/soft coordination environment. The so generated dicationic AE arene complexes are unprecedented and show high and hard Lewis acidities in line with other Lewis superacidic, neutral,[32] mono-[33] and dicationic[31,34] main-group Lewis acids published in recent years.

The coordination by weak neutral σ/π-donors to generate other dicationic complexes is currently explored. However, orienting reactions to explore the coordination chemistry of isolable $[(\eta^6\text{-HMB})Sr(oDFB)_4]^{2+}$ **6** has furthermore shown the sensitivity of this complex; disturbance by strong σ-donors (*e.g.* PPh_3) has shown partial rearrangement of the counterion to form **5** $[(\eta^6\text{-HMB})Sr(oDFB)_3\{f\text{-}al\}]^+$ among other products. Yet, the thereby or directly generated monocationic complexes $[(\eta^6\text{-HMB})M(oDFB)_n\{f\text{-}al\}]^+$ (M = Ca, Sr, Ba) may open interesting reactivities due to stabilization – in the presence of stronger donors – by the potentially hemi-labile [*f-al*]$^-$ moiety bearing an ideal platform for application of this class of compounds for Lewis acid catalyzed transformations, which will be addressed in the future.

Conflicts of interest

The authors declare no conflicts of interest.

Acknowledgements

This work was supported by the Albert-Ludwigs-Universität Freiburg, the Deutsche Forschungsgemeinschaft (KR2046/37-1) and the Carl-Zeiss-Stiftung. We thank Dr H. Scherer and F. Bitgül for performing NMR measurements, Dr T. Ludwig for measuring pXRD, Dr D. Kratzert for help with scXRD measurements, and the Magres Core Facility for instrument support.

Notes and references

‡ Note that $oDFB{\cdot}Al(OR^F)_3$ is unstable in solution at RT over prolonged periods of time as necessary for the syntheses.

1 (*a*) K. Ziegler, H. Froitzheim-Kühlhorn and K. Hafner, *Chem. Ber.*, 1956, **89**, 434; (*b*) R. Zerger and G. Stucky, *J. Organomet. Chem.*, 1974, **80**, 7.
2 L. Bonomo, E. Solari, R. Scopelliti and C. Floriani, *Chem.–Eur. J.*, 2001, **7**, 1322.
3 M. Lindsjö, A. Fischer and L. Kloo, *Dalton Trans.*, 2010, **39**, 1467.
4 (*a*) A. Friedrich, J. Pahl, H. Elsen and S. Harder, *Dalton Trans.*, 2019, **48**, 5560; (*b*) J. Pahl, H. Elsen, A. Friedrich and S. Harder, *Chem. Commun.*, 2018, **54**, 7846; (*c*) J. Pahl, A. Friedrich, H. Elsen and S. Harder, *Organometallics*, 2018, **37**, 2901.
5 J. Pahl, S. Brand, H. Elsen and S. Harder, *Chem. Commun.*, 2018, **54**, 8685.
6 (*a*) M. S. Hill, D. J. Liptrot and C. Weetman, *Chem. Soc. Rev.*, 2016, **45**, 972; (*b*) J. Pahl, T. E. Stennett, M. Volland, D. M. Guldi and S. Harder, *Chem.–Eur. J.*, 2019, **25**, 2025.
7 J. Penafiel, L. Maron and S. Harder, *Angew. Chem., Int. Ed.*, 2015, **54**, 201.
8 S. Brand, H. Elsen, J. Langer, W. A. Donaubauer, F. Hampel and S. Harder, *Angew. Chem., Int. Ed.*, 2018, **57**, 14169.
9 (*a*) M. D. Anker and M. S. Hill, in *Encyclopedia of inorganic and bioinorganic chemistry*, ed. R. A. Scott, Wiley, Chichester, 2012, vol. 475, pp. 1–23; (*b*) H. Bauer, M. Alonso, C. Fischer, B. Rösch, H. Elsen and S. Harder, *Angew. Chem., Int. Ed.*, 2018, **57**, 15177; (*c*) H. Bauer, M. Alonso, C. Färber, H. Elsen, J. Pahl, A. Causero, G. Ballmann, F. de Proft and S. Harder, *Nat. Catal.*, 2018, **1**, 40; (*d*) H. Bauer, K. Thum, M. Alonso, C. Fischer and S. Harder, *Angew. Chem., Int. Ed.*, 2019, **58**, 4248; (*e*) B. Rösch, T. X. Gentner, H. Elsen, C. A. Fischer, J. Langer, M. Wiesinger and S. Harder, *Angew. Chem., Int. Ed.*, 2019, **58**, 5396; (*f*) A. S. S. Wilson, M. S. Hill and M. F. Mahon, *Organometallics*, 2019, **38**, 351; (*g*) M. S. Hill, M. F. Mahon, A. S. S. Wilson, C. Dinoi, L. Maron and E. Richards, *Chem. Commun.*, 2019, **55**, 5732; (*h*) D. Mukherjee, T. Höllerhage, V. Leich, T. P. Spaniol, U. Englert, L. Maron and J. Okuda, *J. Am. Chem. Soc.*, 2018, **140**, 3403; (*i*) D. Schuhknecht, C. Lhotzky, T. P. Spaniol, L. Maron and J. Okuda, *Angew. Chem., Int. Ed.*, 2017, **56**, 12367; (*j*) D. Schuhknecht, T. P. Spaniol, L. Maron and J. Okuda, *Angew. Chem., Int. Ed.*, 2020, 310.
10 M. Schorpp, S. Rein, S. Weber, H. Scherer and I. Krossing, *Chem. Commun.*, 2018, **54**, 10036.
11 (*a*) I. Krossing and A. Reisinger, *Coord. Chem. Rev.*, 2006, **250**, 2721; (*b*) M. Rohde, L. O. Müller, D. Himmel, H. Scherer and I. Krossing, *Chem.–Eur. J.*, 2014, **20**, 1218.
12 A. Martens, P. Weis, M. C. Krummer, M. Kreuzer, A. Meierhöfer, S. C. Meier, J. Bohnenberger, H. Scherer, I. Riddlestone and I. Krossing, *Chem. Sci.*, 2018, **9**, 7058.
13 L. Garcia, M. D. Anker, M. F. Mahon, L. Maron and M. S. Hill, *Dalton Trans.*, 2018, **47**, 12684.
14 M. J. Harvey, D. J. Burkey, S. C. Chmely and T. P. Hanusa, *J. Alloys Compd.*, 2009, **488**, 528.
15 R. A. Williams, T. P. Hanusa and J. C. Huffman, *Organometallics*, 1990, **9**, 1128.
16 M. W. Bouwkamp, P. H. M. Budzelaar, J. Gercama, I. Del Hierro Morales, J. de Wolf, A. Meetsma, S. I. Troyanov, J. H. Teuben and B. Hessen, *J. Am. Chem. Soc.*, 2005, **127**, 14310.
17 (*a*) A. Bihlmeier, M. Gonsior, I. Raabe, N. Trapp and I. Krossing, *Chem.–Eur. J.*, 2004, **10**, 5041; (*b*) A. Martens,

M. Kreuzer, A. Ripp, M. Schneider, D. Himmel, H. Scherer and I. Krossing, *Chem. Sci.*, 2019, **10**, 2821; (*c*) I. Krossing and I. Raabe, *Chem.–Eur. J.*, 2004, **10**, 5017.

18 H. Böhrer, N. Trapp, D. Himmel, M. Schleep and I. Krossing, *Dalton Trans.*, 2015, **44**, 7489.

19 I. D. Brown, *J. Appl. Crystallogr.*, 1996, **29**, 479.

20 T. M. Cameron, C. Xu, A. G. Dipasquale and A. L. Rheingold, *Organometallics*, 2008, **27**, 1596.

21 A. Kraft, N. Trapp, D. Himmel, H. Böhrer, P. Schlüter, H. Scherer and I. Krossing, *Chem.–Eur. J.*, 2012, **18**, 9371.

22 L. O. Müller, D. Himmel, J. Stauffer, G. Steinfeld, J. Slattery, G. Santiso-Quiñones, V. Brecht and I. Krossing, *Angew. Chem., Int. Ed.*, 2008, **47**, 7659.

23 X. Wu, L. Zhao, J. Jin, S. Pan, W. Li, X. Jin, G. Wang, M. Zhou and G. Frenking, *Science*, 2018, **361**, 912.

24 A. E. Reed, R. B. Weinstock and F. Weinhold, *J. Chem. Phys.*, 1985, **83**, 735.

25 C. Ehrhardt and R. Ahlrichs, *Theor. Chim. Acta*, 1985, **68**, 231.

26 (*a*) R. F. W. Bader, *Chem. Rev.*, 1991, **91**, 893; (*b*) T. Lu and F. Chen, *J. Comput. Chem.*, 2012, **33**, 580.

27 U. Mayer, V. Gutmann and W. Gerger, *Monatsh. Chem.*, 1975, **106**, 1235.

28 A. Klamt and G. Schüürmann, *J. Chem. Soc., Perkin Trans. 2*, 1993, **2**, 799.

29 L. Greb, *Chem.–Eur. J.*, 2018, **24**, 17881.

30 (*a*) J. M. Bayne and D. W. Stephan, *Chem. Soc. Rev.*, 2016, **45**, 765; (*b*) E. R. Clark and M. J. Ingleson, *Organometallics*, 2013, **32**, 6712; (*c*) V. Fasano, J. H. W. LaFortune, J. M. Bayne, M. J. Ingleson and D. W. Stephan, *Chem. Commun.*, 2018, **54**, 662; (*d*) J. Zhou, L. L. Liu, L. L. Cao and D. W. Stephan, *Angew. Chem., Int. Ed.*, 2019, **58**, 5407; (*e*) E. R. Clark, A. Del Grosso and M. J. Ingleson, *Chem.–Eur. J.*, 2013, **19**, 2462; (*f*) J. M. Slattery and S. Hussein, *Dalton Trans.*, 2012, **41**, 1808; (*g*) B. Pan and F. P. Gabbaï, *J. Am. Chem. Soc.*, 2014, **136**, 9564; (*h*) C. B. Caputo, L. J. Hounjet, R. Dobrovetsky and D. W. Stephan, *Science*, 2013, **341**, 1374; (*i*) C. B. Caputo, D. Winkelhaus, R. Dobrovetsky, L. J. Hounjet and D. W. Stephan, *Dalton Trans.*, 2015, **44**, 12256.

31 P. Mehlmann, T. Witteler, L. F. B. Wilm and F. Dielmann, *Nat. Chem.*, 2019, **11**, 1139.

32 R. Maskey, M. Schädler, C. Legler and L. Greb, *Angew. Chem., Int. Ed.*, 2018, **57**, 1717.

33 (*a*) H. Zhao and F. P. Gabbaï, *Nat. Chem.*, 2010, **2**, 984; (*b*) P. Weis, D. C. Röhner, R. Prediger, B. Butschke, H. Scherer, S. Weber and I. Krossing, *Chem. Sci.*, 2019, **10**, 10779.

34 J. Zhou, L. L. Liu, L. L. Cao and D. W. Stephan, *Chem*, 2018, **4**, 2699.

